Research Square

Preprints are preliminary reports that have not undergone peer review.
They should not be considered conclusive, used to inform clinical practice,
or referenced by the media as validated information.

Clinical and genomic evaluation of Plasmodium falciparum Exported protein 1 for malaria diagnosis

Kailash (C) Pandey

kailash.pandey@icmr.gov.in

National Institute of Malaria Research, New Delhi, India https://orcid.org/0000-0003-3936-4357

Hem Singh

ICMR-National Institute of Malaria Research

Bhuvan Dixit

ICMR-National Institute of Malaria Research

Vikas Kumar

ICMR-National Institute of Malaria Research

Anitha Bavikatte

Institute of Bioinformatics and Applied Biotechnology

Padmini Nayak

ICMR-National Institute of Malaria Research

Nishtha Tiwari

ICMR-National Institute of Malaria Research

Soumyananda Chakraborti

Birla Institute of Technology and Science, Pilani Hyderabad Campus

Ram Das

ICMR-National Institute of Malaria Research

Byoung Na

Gyeongsang National University, College of Medicine

Richa Singhal

ICMR-National Institute of Malaria Research

Shailja Singh

Jawaharlal Nehru University https://orcid.org/0000-0001-5286-6605

Shruthi S Vembar

https://orcid.org/0000-0002-7497-6378

Praveen Kumar Tripathi

ICMR - NAtional Institute of Malaria Research

Kapil Vashisht

ICMR-National Institute of Malaria Research https://orcid.org/0000-0003-0550-0162

Article

Keywords: P. falciparum, Exported protein 1, polyclonal antibodies, monoclonal antibodies, western blot, sensitivity, specificity, ROC curve, Training and validation subsets, Epitope, HRP2/3 gene deletions, Rapid diagnostic test (RDT) failures, Global genetic diversity

Posted Date: November 18th, 2026

DOI: https://doi.org/10.21203/rs.3.rs-11612823/v1

License: This work is licensed under a Creative Commons Attribution 4.0 International License.
Read Full License

Additional Declarations: There is **NO** Competing Interest. None

Clinical and genomic evaluation of *Plasmodium falciparum* Exported protein 1 for malaria diagnosis

Hem Lata Singh[1,2], Bhuvan Dixit[1], Vikas Kumar[1,2], Anitha Nagaraj Bavikatte[3], Padmini Nayak[1], Nishtha Tiwari[1,2], Soumyananda Chakraborti[4], Ram Das[1,2], Byoung-Kuk Na[5], Richa Singhal[1,2], Shailja Singh[6], Shruthi Sridhar Vembar[3], Praveen K Tripathi[1,2], Kapil Vashisht[1]*, Kailash C Pandey[1,2]*

[1]ICMR-National Institute of Malaria Research, New Delhi, Delhi - 110077, India
[2]Academic of Scientific and Innovative Research (AcSIR) Ghaziabad, Uttar Pradesh - 201002, India
[3]Institute of Bioinformatics and Applied Biotechnology, Bengaluru, Karnataka - 560100, India
[4]Birla Institute of Technology and Science, Pilani Hyderabad Campus, Jawahar Nagar, Kapra Mandal Telangana – 500078, India
[5]Gyeongsang National University, College of Medicine, Jinju – 52828, South Korea
[6]Special Center for Molecular Medicine, Jawaharlal Nehru University, New Delhi, Delhi – 110067, India

Correspondence: kailash.pandey@icmr.gov.in; vashisht.kapil07@gmail.com

Abstract

The increasing prevalence of *Plasmodium falciparum* parasites carrying Pf*hrp2/3* deletions threatens the reliability of PfHRP2-based rapid diagnostic tests (RDTs), particularly in the malaria-endemic regions. This study clinically evaluated native PfEXP1 (nPfEXP1) as a candidate diagnostic biomarker and investigated its global genetic diversity. Polyclonal and monoclonal anti-PfEXP1 antibodies detected nPfEXP1 in cultured parasites at estimated amounts of 0·14 and 0·014 ng, respectively. Monoclonal antibodies also detected nPfEXP1 in cultured parasites carrying Pf*hrp2* or Pf*hrp2/3* deletions. In a cross-sectional Phase II biomarker evaluation involving 121 *P. falciparum*-positive samples and 80 malaria-negative controls from India, indirect ELISA demonstrated significantly higher nPfEXP1 reactivity in the parasite density-segregated infected samples than in the controls ($p<0·0001$). The cohort was randomly divided into training and validation subsets in a 70:30 ratio. At the training-derived cutoff, the PfEXP1 index assay achieved 86% sensitivity (95% CI, 71–95) and 58% specificity (95% CI, 37–78) in the validation subset, compared with 95% sensitivity (95% CI, 82–99) and 88% specificity (95% CI, 69–96) for the PfHRP2 comparator assay. Analysis of the MalariaGEN Pf8 dataset revealed geographically clustered PfEXP1 polymorphisms, including recurrent variations at amino acid positions 136 and 160, while the examined epitope region remained largely conserved. These findings support PfEXP1 as a potential complementary diagnostic antigen and provide a basis for developing monoclonal antibody-based sandwich assays and evaluating their performance in larger, geographically diverse clinical cohorts.

Keywords: *P. falciparum*, Exported protein 1, polyclonal antibodies, monoclonal antibodies, western blot, sensitivity, specificity, ROC curve, Training and validation subsets, Epitope, HRP2/3 gene deletions, Rapid diagnostic test (RDT) failures, Global genetic diversity

1. Introduction

According to the World Malaria Report 2025, an estimated 282 million malaria cases and approximately 0.6 million associated deaths occurred worldwide in 2024, reflecting an increase of nearly 9 million cases compared with 2023[1]. Accurate and timely diagnosis is central to effective malaria control and elimination strategies. Immunochromatography based Rapid diagnostic tests (RDTs) have become indispensable tools to detect malaria infections globally, owing to their ease of use and rapid turnaround. Rapid diagnostic tests (RDTs) for *Plasmodium falciparum* primarily rely on the detection of histidine-rich proteins 2 and 3 (PfHRP2 and PfHRP3), while alternative assays target pan-*Plasmodium* or species-specific antigens, including parasite lactate dehydrogenase (pLDH) and aldolase[2]. PfHRP2-based RDTs demonstrate higher diagnostic sensitivity (~96·3%) than pLDH-based assays (~82·6%); however, their diagnostic reliability is undermined by several critical limitations[3]. Importantly, PfHRP2 may persist in circulation even after treatment and can lead to false positive results in RDTs; while expanding deletions in the Pf*hrp2/3* genes in field isolates drive false negatives and delayed treatment[4]. Field evaluations from South Sudan showed high sensitivity for both HRP2 and pLDH RDTs (>99%), but low specificity of ~61.7% and 55%, respectively, indicating high false-positive rates. Similarly, in Yemen, combined HRP2/pLDH RDTs exhibited specificity as low as ~56%, which further decreased to ~30% among previously treated individuals, further highlighting inconsistent real-world performance, with reduced specificity under endemic conditions[5,6]. The WHO Malaria Threats Map reports Pf*hrp2/3* deletions in 40 of 47 surveyed countries marking a severe threat upon the global diagnostic reliability of PfHRP2 based RDTs[7]. In the most severely affected regions, false-negative rates of up to 80% have been observed due to Pf*hrp2* deletions[8] **(Table 1)**. Eritrea, for instance, has one of the highest reported prevalences of Pf*hrp2/3* deletions globally, with estimates exceeding 50-60% and reaching as high as 62% overall and 80% in some hospitals[9]. Nonetheless, reported deletion frequencies vary substantially across Africa, from 1.45% in Mozambique and 0.4% in Angola to approximately 5% in Uganda, 36% in Ghana, and 22% in Democratic Republic of Congo[10-13]. While, the overall prevalence of Pf*hrp2* deletions in India remains relatively low (2-5%); regional heterogeneity has been reported[14]. Pf*hrp2* gene deletions in Odisha were identified in 65.5% of RDT-negative, microscopy-confirmed infections[15]. Considerable efforts have been directed toward identifying alternative biomarkers, including glutamate dehydrogenase (GDH), merozoite surface proteins (MSP2), glutamate-rich protein (GLURP) and specific serine/threonine protein kinases (chimeric-FIKK)[16-18].

However, their translational potential through clinical evaluation studies remains limited due to significant antigenic polymorphisms, variability in expression levels, and inconsistent performance across geographically diverse parasite populations[19,20] field-deployable RDTs. These limitations collectively underscore the urgent need for next-generation diagnostic markers that combine high sensitivity, improved specificity, and robustness across diverse epidemiological settings.

In our previous work, we identified a cyclic peptide of *P. falciparum* Exported Protein-1 (PfEXP1) demonstrating strong immunoreactivity with *P. falciparum* infected patient sera, suggesting its diagnostic potential[21]. PfEXP1 is a highly conserved, membrane-associated protein localized to the parasitophorous vacuole membrane (PVM) and is essential for parasite survival during intraerythrocytic stages[22-24]. Importantly, PfEXP1 is abundantly and consistently expressed during blood stages and exhibits relatively low sequence variability compared to surface antigens, making it less susceptible to immune evasion and genetic deletion[25-27]. Furthermore, PfEXP1 elicited robust $CD4^+$ T cell responses, indicating its immunological relevance and potential as a biomarker of parasite exposure[22,27,28]. It exhibits glutathione S-transferase (GST)-like activity, contributing to redox homeostasis and protection against oxidative stress within the host erythrocyte[23,29]. Structurally, PfEXP1 spans the PVM with defined orientation, facilitating interactions with key transport proteins such as PfEXP2, thereby supporting nutrient exchange and parasite growth[23,26]. Functional studies have demonstrated that disruption of PfEXP1 leads to severe defects in PVM integrity and parasite viability, highlighting its critical role in parasite biology[23].

In this Phase II biomarker evaluation study, we report, to our knowledge, the first clinical evaluation of PfEXP1 as a candidate malaria diagnostic biomarker in a substantial Indian cohort comprising 121 *P. falciparum*-positive patients with quantified parasitaemia and 80 malaria-negative controls. Beyond the established diagnostic antigens PfHRP2, parasite lactate dehydrogenase (pLDH), and aldolase, relatively few alternative parasite-derived antigens have undergone clinical evaluation in cohorts of this scale. We characterized the detectability of native PfEXP1 (nPfEXP1) in cultured parasite lysates and assessed its diagnostic performance using a polyclonal antibody-based indirect ELISA, with PfHRP2 ELISA serving as the comparator assay. The findings of this study highlight the promise of PfEXP1 as a candidate antigen for malaria diagnosis. Further development and optimization of the identified monoclonal antibody pair are expected to facilitate the development of an advanced PfEXP1-targeted sandwich immunoassay, potentially improving its diagnostic performance and supporting its future clinical translation. Collectively, these findings establish a foundation for

further evaluation of PfEXP1 as a complementary diagnostic target and its potential incorporation into next-generation malaria diagnostic platforms, particularly in regions affected by Pf*hrp2/3* deletions.

2. Results

2.1 Clinical evaluation of PfEXP1 as a candidate diagnostic biomarker

2.1.1 Characterization of rPfEXP1

Comparative sequence analysis of PfEXP1 and its orthologues in other human-infecting *Plasmodium* species (*P. vivax*, *P. ovale*, *P. malariae*, and *P. knowlesi*) together with the domain architecture of PfEXP1 is presented in detail in supplementary results **section 2.1 (Figs. 1A, 1B, S1A-C)**. Recombinant PfEXP1 (rPfEXP1) production, thermal stability assessment, and generation of polyclonal anti-PfEXP1 antibodies (pAb-PfEXP1) are described in supplementary results section **2.2 (Figs. 1C and 1D)**. The generated pAb-PfEXP1 successfully recognized rPfEXP1 at its expected molecular weight of approximately 23 kDa **(Fig. 1E)**. The oligomeric state, secondary structure, and folding characteristics of rPfEXP1 were further investigated using size exclusion chromatography and circular dichroism (CD) spectroscopy, while its biological activity was assessed using a glutathione S-transferase (GST) functional assay **(Figs. S2A–C)**; supplementary results section **2.2**. To determine the analytical detection limit of rPfEXP1, serial dilutions of the protein (10–0.078 ng) were spotted onto a nitrocellulose membrane and analysed by dot blot assay. The polyclonal anti-PfEXP1 antibody (pAb-PfEXP1) detected rPfEXP1 at amounts as low as 0.625 ng, establishing the lowest detectable protein amount under the assay conditions **(Fig. 1G)**.

2.1.2 Semiquantitative estimation of native PfEXP1 in cultured *P. falciparum* parasite lysates

Native PfEXP1 (nPfEXP1) was detected across the asexual intraerythrocytic developmental stages of the *P. falciparum* 3D7 strain using pAb-PfEXP1 antibodies. Western blot analysis of stage-specific parasite lysates (3 µg per lane) confirmed the presence of nPfEXP1 in ring, trophozoite, and schizont stages, indicating its expression throughout the asexual blood-stage development of *P. falciparum* **(Fig. 1F)**. The abundance of nPfEXP1 in cultured *P. falciparum* parasite lysates from two strains Pf3D7 and PfJDP8 (a culture-adapted field isolate) was estimated semiquantitatively using rPfEXP1 as a reference standard. The amount of parasite lysate loaded in each lane of the dot blot and Western blot lane was determined, and the corresponding nPfEXP1 content was indirectly estimated using a calibration curve generated

from rPfEXP1-based indirect ELISA measurements. A linear relationship [$y = 0.1273 \ln(x) + 0.3834$] was observed between the immunoreactive signal intensity and the logarithm of rPfEXP1 quantity, enabling estimation of nPfEXP1 abundance in parasite lysates **(Table S2 and S3)**. nPfEXP1 was estimated at approximately 0.14 ng in lysates containing ~1×10^5 Pf3D7 parasites, as determined by both dot blot and Western blot analyses **(Fig. S3 and Fig. 2A)**. Similarly, the nPfEXP1 content in lysates corresponding to ~1×10^5 parasites of the PfJDP8 strain was estimated to be 0·14 ng **(Fig. 2B)**.

2.1.3 Diagnostic performance of PfEXP1 (index) and PfHRP2 (comparator) assays

The diagnostic performance of PfEXP1 (index assay) and PfHRP2 (comparator assay) was evaluated in 121 microscopy- and RDT-confirmed *P. falciparum*-positive samples. Both assays were evaluated against a common control group comprising 74 *P. falciparum*-negative individuals from the same malaria-endemic region and six healthy individuals from a non-endemic region (n=80). Based on parasite density, positive samples were stratified into three groups: low (<5,000 parasites/µl), moderate (5,000–100,000 parasites/µl), and high (>100,000 parasites/µl) parasitaemia. Demographic and clinical characteristics of the study participants are provided in the supplementary information **(Table S1)**. The median parasite densities for both the cohorts were 11,564 parasites/µl (Interquartile range (IQR): 29,994) in the overall infected group, with corresponding values of 2,090 (IQR: 2,650), 16,661 (IQR: 22,732), and 1,65,110 (IQR: 1,02,972) parasites/µl across the low, moderate, and high parasitaemia groups, respectively **(Table S1)**. Box-and-whisker plots were generated to compare OD_{450} values across five groups: uninfected controls, total infected samples, and low, moderate, and high parasitaemia subgroups for both the index and comparator assays. Statistical comparisons were performed using unpaired t-tests with Welch's correction, in each infected group and control group separately. In both assays, OD_{450} values differed significantly between uninfected controls and each infected group, including the three parasitaemia subgroups ($p < 0·001$) **(Fig. 3A and 3B)**.

Receiver operating characteristic (ROC) curve analysis was performed to assess the discriminatory performance of the index (PfEXP1) and comparator (PfHRP2) assays across the complete study cohort. The area under the curve (AUC) was calculated using malaria-negative and various groups of malaria-positive samples, as described previously. The index assay (nPfEXP1) demonstrated consistent diagnostic performance across parasitaemia groups, with AUC values of 0·88 (95% CI: 0·84–0·93) for the overall infected cohort, 0·89 (0·83–0·94) for low, 0·89 (0·84–0·94) for moderate, and 0·84 (0·72–0·96) for high parasitaemia groups **(Fig.**

4A). In comparison, the PfHRP2-based comparator assay demonstrated fairly better discriminatory performance, with AUC values of approximately 0·98 across all parasitaemia groups **(Fig. 4B)**. For the PfEXP1 index assay, the optimal diagnostic cutoff (OD_{450} = 0·3412), determined using the 70% training subset (n=140; 84 malaria-positive and 56 malaria-negative samples), yielded a sensitivity of 90% and specificity of 77%. The corresponding 2×2 contingency table comprised 76 true positives (TP), 13 false positives (FP), 8 false negatives (FN), and 43 true negatives (TN). When this predefined cutoff was applied to the 30% validation subset (n=61; 37 malaria-positive and 24 malaria-negative samples), the assay achieved a sensitivity of 86% and specificity of 58%, with 32 TP, 10 FP, 5 FN, and 14 TN **(Table 2 & 3)**. For the PfHRP2 comparator assay, the optimal diagnostic cutoff (OD_{450} = 0·1145), derived from the 70% training subset (n=140; 84 malaria-positive and 56 malaria-negative samples), yielded a sensitivity of 100% and specificity of 91%. The corresponding contingency table comprised 84 TP, 5 FP, 0 FN, and 51 TN. Application of this training-derived cutoff to the 30% validation subset (n = 61; 37 malaria-positive and 24 malaria-negative samples) resulted in a sensitivity of 95% and specificity of 88%, with 35 TP, 3 FP, 2 FN, and 21 TN **(Table 2 & 3)**. In the validation subset, the negative predictive values (NPVs) were 74% for PfEXP1 and 91% for PfHRP2, whereas the corresponding positive predictive values (PPVs) were 76% and 92%, respectively. Overall diagnostic accuracy was 75% for the PfEXP1 assay and 91% for the PfHRP2 comparator assay.

2.1.4 Detection and estimation of native PfEXP1 by Western blotting using mAb-PfEXP1

The monoclonal antibody against PfEXP1 (mAb-PfEXP1; clone 3B3B2) was generated as described in supplementary methods section **1.5**, and evaluated for its ability to detect nPfEXP1 in cultured *P. falciparum* parasite lysates by Western blotting. Lysates prepared from approximately 1×10^8 parasites were serially diluted, as detailed in **Table S4**. The antibody detected nPfEXP1 over a parasite-equivalent range of 4×10^6 to 1×10^4 parasites, corresponding to estimated nPfEXP1 amounts of 5·63 to 0·014 ng, respectively **(Fig. 5A)**. The lowest detectable parasite-equivalent load in this experiment was 1×10^4 parasites, corresponding to an estimated 0·014 ng of nPfEXP1.

In a separate Western blot experiment, mAb-PfEXP1 detected nPfEXP1 in serially diluted *P. falciparum* lysates at a lowest parasite-equivalent load of approximately 8×10^3 parasites, corresponding to an estimated 0·014 ng of nPfEXP1 **(Fig. 5B; Table S5)**. Recombinant PfEXP1 (rPfEXP1) was included as a positive control. No detectable cross-reactivity was observed with the pooled *P. vivax*-infected erythrocyte lysate containing approximately 50,000

parasites, indicating the absence of a detectable signal with mAb-PfEXP1 under the experimental conditions **(Fig. 5B)**.

2.1.5 Detection of nPfEXP1 in Pf*hrp2/3* deleted parasites and culture adapted Indian field isolate of *P. falciparum*

To investigate whether nPfEXP1 remains detectable in *P. falciparum* parasites harbouring Pf*hrp2/3* deletions, Δ*hrp2* and Δ*hrp2/3* mutant parasite lines were cultured as described in supplementary methods section **1.4**. Western blot analysis using mAb-PfEXP1 successfully detected nPfEXP1 in lysates from the wild-type Pf3D7 and PfJDP8 strains, as well as both deletion mutant lines, whereas uninfected erythrocytes, included as a negative control, showed no detectable signal **(Fig. 6)**. The Pf*hrp2* deletion status was further examined by PCR using exon 2-specific primers. Amplification was observed in Pf3D7 and PfJDP8 but was absent in both Δ*hrp2* and Δ*hrp2/3* mutant lines, consistent with the absence of the Pf*hrp2* locus. The no-template control showed no amplification **(Fig. 6, inset)**. These findings demonstrate that nPfEXP1 remains detectable in Pf*hrp2*-deficient parasites, supporting its potential as an alternative diagnostic target for overcoming Pf*hrp2* deletion-associated RDT failures.

2.2 Global population genetic diversity and protein polymorphisms of PfEXP1

To evaluate the global, naturally occurring genetic diversity at the Pf*exp1* genomic locus, we utilized the MalariaGEN Pf8 repository[30], which contains high-quality variant-calling data for 24,409 *P. falciparum* isolates from 99 whole genome sequencing (WGS) partner studies spanning 34 malaria-endemic countries, including 316 samples collected across three Indian states (Tripura, Odisha, and West Bengal). Analysis of biallelic variant calls within the Pf*exp1*-encoding locus (PF3D7_1121600; located on chromosome 11 (coordinates: 814,343–818,094 [-])), identified 273 single nucleotide variants (SNVs), 34 insertions and 38 deletions. The largest proportion of the SNVs were located within exons (101 variants; 37.0%), followed by 3′ untranslated (UTR)/downstream regions (74; 27.1%), 5′ UTR/upstream regions (66; 24.2%), and introns (32; 11.7%) **(Fig. 7A)**. Moreover, functional annotation of the coding variants revealed that a majority were missense substitutions (74/101; 73.3%), followed by 23 variants (22.8%) that were synonymous **(Fig. 7B)**; only four high-impact variants were detected, comprising two stop-gained mutations and one each of start-lost and stop-retained variants, indicating that disruptive mutations within PfEXP1 are rare in natural parasite populations, in keeping with this gene's essentiality for parasite intra-erythrocytic development[31].

Thereafter, to determine the amino acid substitutions that arise from the 74 missense variants in the PfEXP1 coding sequence, as well as the resultant haplotypes and their global distribution,

we analysed pre-processed data for 18,970 *P. falciparum* isolates from Pf-HaploAtlas[32]. Among 81 identified protein haplotypes carrying one to four amino acid substitutions, 23 met our threshold of being present in at least 10 quality-controlled isolates and were selected for downstream analysis. Mapping the associated amino acid substitutions onto the primary structure of PfEXP1 revealed that the mutations are non-randomly clustered along the protein sequence **(Fig. 7C)**, i.e., a distinct substitution hotspot was observed near the N-terminal region (comprising S31N, V33I, and S34N), whereas the highest density of sequence variation clustered within the C-terminal region which is exposed to the host erythrocyte cytoplasm (including I112L, N115K, N130H, G136D/V, P137T, V144A, G159V, and T160P/S). A closer look at haplotype frequency indicated that the G136D+T160P haplotype is most prevalent in the MalariaGEN Pf8 dataset (5,894 isolates; 31.1%) followed by I112L+G136D (3,627 isolates; 19.1%), T160P (2,936 isolates; 15.5%), and G136V (1,914 isolates; 10.1%), with the reference haplotype of the *P. falciparum* 3D7 strain found in just 1134 isolates. Furthermore, the haplotypes demonstrate distinct geographic structure across malaria-endemic regions **(Fig. 7D and 7E)**. The G136+T160P haplotype dominates in Eastern South-East Asia (AS-SE-E), Oceania (OC-NG) and India (AS-S-E), followed by the T160P haplotype which is dominant in Western South-East Asia (AS-SE-W) and Far-Eastern South Asia (AS-S-FE). In contrast, the predominant haplotype in three African regions, North-Eastern (AF-NE), Eastern (AF-E), and Central (AF-C) Africa, is I112L+G136D, followed by T160P and G136V, while in Western Africa (AF-W), G136V, T160P and N130H+G136D are the most prevalent haplotypes, in decreasing order of frequency. Notably, South American regions have two more or less equidominant haplotypes, T160P and G136V. Overall, amino acid positions 136 (13 of 21 haplotypes) and 160 (16 of 21 haplotypes) emerged as the most variable in the MalariaGEN Pf8 dataset. A similar trend was observed in a second independent WGS dataset generated through the ICEMR-MESA program for 50 Indian *P. falciparum* strains[33,34], with 35 samples harboring the T160P haplotype, three bearing the G136D+T160P haplotype, three bearing S31N+T160P haplotype, two S34N+G136D+T160P and one each the G136D, I112L+G136D, S31N+I112L+G136D and S34N+T160P haplotypes **(Table S5)**.

3. Discussion

A candidate diagnostic biomarker should exhibit consistent expression across clinically relevant parasite stages, sufficient abundance for reliable detection, and adequate diagnostic sensitivity and specificity to distinguish infected from uninfected individuals. Accordingly, PfEXP1 was evaluated against these key criteria. First, nPfEXP1 was consistently detected

across the asexual blood stages of *P. falciparum*, including rings, trophozoites, and schizonts, supporting its suitability for detecting infections irrespective of the predominant circulating parasite stage. Second, immunoblotting with pAb-PfEXP1 antibodies demonstrated detectable nPfEXP1 in lysates from both the Pf3D7 reference strain and the culture-adapted Indian field isolate PfJDP8, with an estimated antigen abundance of 0·14 ng rPfEXP1 equivalents at the lowest detectable parasite load. mAb-PfEXP1 antibodies enabled detection at a lower parasite-equivalent load in Pf3D7 lysates, corresponding to an estimated 0·014 ng rPfEXP1 equivalents; demonstrating the detectability of native PfEXP1 across parasite strains and highlight the potential of monoclonal antibodies for sensitive antigen detection. Thirdly, the clinical evaluation using a matched cohort of 121 *P. falciparum*-positive samples and 80 malaria-negative controls, the PfEXP1 indirect ELISA demonstrated a sensitivity of 90% and specificity of 77% in the training subset. When the training-derived cutoff was applied unchanged to the validation subset, the assay retained a relatively high sensitivity of 86%, although specificity decreased to 58%. The reduced specificity may reflect non-specific binding of the polyclonal pAb-PfEXP1 antibodies to components of erythrocyte lysates or other sample-associated factors. The paired monoclonal antibodies identified and currently under sandwich assay development might be helpful in improving the specificity. The development of a sandwich ELISA using a pair of monoclonal antibodies recognizing distinct, non-overlapping epitopes of PfEXP1. Such a format could improve target-specific antigen capture and detection while reducing signals arising from non-specific interactions[35]. Notably, the PfHRP2 comparator assay, evaluated using the same clinical cohort, achieved approximately 95% sensitivity and 88% specificity in the validation subset using an indirect ELISA format. This comparison highlights the scope for further optimization of the PfEXP1 assay. However, the anticipated improvement in diagnostic performance through a sandwich format will need to be established experimentally. Taken together, these findings strongly suggest that developing a mAb-mAb sandwich ELISA for nPfEXP1 will provide the necessary analytical gain to elevate its diagnostic sensitivity and specificity across the full spectrum of clinical parasitemia. An important observation was the detection of nPfEXP1 in *P. falciparum* parasites carrying Pf*hrp2/3* gene deletions using mAb-PfEXP1, demonstrating that nPfEXP1 could be detected despite the absence of these loci and supporting its potential as an alternative diagnostic target in parasites with Pf*hrp2/3* deletions.

The clinical evaluation was conducted in a malaria-endemic region of Jharkhand, India, where malaria transmission is predominantly seasonal. Very low parasitaemia (<1,000 parasites/μL)

and very high parasite densities were relatively uncommon in the study population. This distribution is consistent with the parasite-density profile observed in a seasonal transmission setting, although transmission intensity cannot be inferred from parasite density alone. The sensitivity of 86% achieved by the nPfEXP1-based indirect ELISA in the validation subset suggests promising diagnostic potential in this population. Further improvement in assay performance, particularly specificity, may be achievable through development of a sandwich ELISA using the candidate paired monoclonal antibodies identified in this study, which is currently underway. Importantly, approximately 73% of the malaria-negative controls recruited from the endemic region presented with fever but tested negative for malaria by both RDT and microscopy. The inclusion of these febrile individuals provided a clinically relevant assessment of assay specificity in a population in which fever could arise from non-malarial causes. Nevertheless, the moderate specificity observed for the pAb-PfEXP1-based assay in the validation subset (58%) indicates that further assay optimization is required. Evaluation in larger and clinically diverse populations, including patients with confirmed non-malarial febrile illnesses, will be important to establish the clinical specificity and broader diagnostic utility of PfEXP1.

Against the backdrop of emerging Pf*hrp2/3* deletions and their implications for malaria diagnosis across the Global South, our analysis of global Pf*exp1* genetic diversity provides important insights into the geographical distribution of PfEXP1 polymorphisms and their potential diagnostic relevance. Distinct regional patterns were observed, with the G136D + T160P haplotype predominating in South and Southeast Asia, including India, whereas the I112L + G136D haplotype was more prevalent in Africa. In contrast, T160P- and G136V-containing haplotypes were prominent in South America. Notably, the G136D substitution lies within a highly immunoreactive region spanning amino acid residues 130–155, previously identified by our group through peptide microarray analysis[21]. The potential effects of this substitution on anti-PfEXP1 antibody binding remain to be experimentally determined. In particular, further studies are warranted to assess whether amino acid polymorphisms at positions 136 and 160 influence antibody recognition and the diagnostic performance of PfEXP1-based assays.

The potential cross-reactivity of the nPfEXP1 index assay with *P. vivax* was assessed using four pooled whole-blood samples containing approximately 50,000 *P. vivax* parasites/µl. No detectable cross-reactive signal was observed, suggesting that the pAb-PfEXP1-based assay exhibits a degree of species specificity for *P. falciparum*. However, this finding should be

interpreted cautiously because of the limited number of pooled samples tested. Cross-reactivity with other human-infecting *Plasmodium* species and the performance of the assay in mixed-species infections were not evaluated in this study and warrant investigation in future validation studies. Sequence comparison further indicated that the PfEXP1 region spanning amino acid residues 129–154 is unique to *P. falciparum*, although shorter conserved sequence regions are present in *P. vivax* and other human-infecting *Plasmodium* species. Notably, a cyclized peptide (NGEPNAGPQVTAQ) derived from this unique C-terminal region exhibited strong reactivity with sera from patients with *P. falciparum* infection but not with sera from *P. vivax*-infected patients in a previous study[21]. Together, these findings support the potential of the C-terminal region of PfEXP1 as a species-discriminating antigenic target. Nevertheless, its specificity requires further confirmation using larger and well-characterized panels of samples from patients infected with *P. vivax*, other human-infecting *Plasmodium* species, and mixed-species infections.

Highlighting the advantages of PfEXP1 over PfHRP2 is essential, particularly regarding post-treatment persistence and gene deletions. A primary limitation of PfHRP2 is its highly secretory nature, which leads to prolonged persistence in circulation and within pitted erythrocytes for up to 40 days post-parasite clearance[36]. This persistence frequently results in false-positive diagnostic outcomes, compromising test accuracy during follow-up. Furthermore, the emerging global prevalence of Pf*hrp2/3* gene deletions poses a severe threat to diagnostic reliability by driving false-negative results. In contrast, nPfEXP1 is an integral membrane protein localized to the PVM. Because it is tightly associated with active, intact intraerythrocytic parasites, its detection reflects the presence of viable infection, thereby substantially reducing false-positive rates. Additionally, given its essential role in parasite survival and nutrient transport across the PVM, spontaneous deletion of nPfEXP1 is highly improbable, offering a sustainable diagnostic alternative immune to the gene deletion issues afflicting PfHRP2. Due to its biochemical and structural stability, constitutive expression during the blood stage, strong immunogenicity with polyclonal and monoclonal, and continued expression in Δ*hrp2/3*-deleted parasite strains, PfEXP1 may represent a promising alternative to HRP2 for malaria diagnosis.

4. Materials and methods

4.1 Study design and participants

This cross-sectional Phase II biomarker evaluation study assessed the clinical diagnostic performance of PfEXP1 as a candidate biomarker for *P. falciparum* malaria and was conducted and reported in accordance with the Standards for Reporting Diagnostic Accuracy Studies (STARD 2015) guidelines[37]. Ethical approval for the collection of patient blood samples was obtained from the Institutional Ethics Committee (IEC) of ICMR–National Institute of Malaria Research (ICMR-NIMR), New Delhi (NIMR/IEC-M/2023/970/v5-Jan/03). Clinical blood samples were collected from individuals residing in the malaria-endemic region of Chaibasa, Jharkhand, India, through the ICMR-NIMR Field Unit, Ranchi, between October 2024 and August 2026.

Inclusion criteria: Individuals presenting with malaria-like symptoms were enrolled and screened for *P. falciparum* infection using a PfHRP2-based rapid diagnostic test (STANDARD Q Malaria Pf/Pv Rapid Test, SD Biosensor Healthcare, India) and microscopic examination by a trained microscopist. Individuals testing positive for *P. falciparum* by RDT were classified as malaria-positive and included in the infected cohort, whereas RDT-negative individuals were classified as malaria-negative and included in the control cohort.

Exclusion criteria: Individuals who did not consent for blood sample collection and contained other human *Plasmodium* infections (*P. vivax*) or mixed infections (Pf & Pv) were excluded from the study.

Whole blood samples (1–3 mL) were collected from 121 *P. falciparum*-positive individuals and 74 malaria-negative individuals residing in a malaria-endemic region, following written informed consent and in accordance with approved ethical guidelines. Additionally, six apparently healthy, asymptomatic individuals from a non-endemic region in Delhi, India, were enrolled as controls after obtaining informed consent. Dried blood spots (DBS) were prepared from all malaria-positive samples using sterile filter paper for subsequent molecular investigations. Parasite densities were determined by thick blood smear microscopy and categorized as low (<5,000 parasites/µl), moderate (5,000–100,000 parasites/µl), or high (>100,000 parasites/µl) parasitaemia. All *P. falciparum*-positive and malaria-negative samples were transported to the ICMR–National Institute of Malaria Research, New Delhi, for further processing and analysis. No formal a priori sample size calculation was performed, as recruitment was constrained by the availability of microscopy-confirmed malaria cases at the

study site. Accordingly, the study was designed as an exploratory Phase II diagnostic biomarker evaluation, with sample size determined by field recruitment feasibility. The demographic and parasitological characteristics of the study participants are summarized in **Table S1**. Whole-blood samples from four *P. vivax*-infected patients (n=4) were obtained from the clinical facility at ICMR–NIMR, New Delhi. The samples had a cumulative parasite density of approximately 50,000 parasites/µl. These samples were included to assess potential cross-reactivity of the monoclonal anti-PfEXP1 antibody with *P. vivax* infected samples.

4.2 Heterologous expression, structural and functional characterization of recombinant PfEXP1, and generation of polyclonal antibodies

Sequence analysis of PfEXP1 was performed to characterize its molecular features and identify conserved regions. The Pf*exp1* coding sequence, excluding the N-terminal 22 amino acids, was cloned and heterologously expressed to produce recombinant PfEXP1 (rPfEXP1), as detailed in supplementary methods section **1.1**. Purified rPfEXP1 was characterized by size-exclusion chromatography and circular dichroism (CD) spectroscopy to assess its oligomeric state and secondary structural characteristics, respectively (supplementary methods section **1.2**). GST-The functional activity of rPfEXP1 was evaluated using a glutathione S-transferase (GST)-like catalytic activity assay described in supplementary methods section **1.2**. Rabbit polyclonal antibodies against PfEXP1 (pAb-PfEXP1) were subsequently generated and evaluated for their ability to recognize both recombinant and native PfEXP1 (nPfEXP1), as described in supplementary methods section **1.3**.

4.3 Preparation of parasite lysates from in vitro-cultured *P. falciparum* and clinical blood samples

For preparation of in vitro-cultured *P. falciparum* lysates, 10 mL of parasite culture at 5% parasitaemia and 4% haematocrit, containing approximately 1×10^8 parasites, was used. For clinical samples, 1 ml of whole blood from *P. falciparum*-positive patients, malaria-negative individuals, and healthy controls was centrifuged at 2,500g for 15 min at 4 °C to separate plasma. The erythrocyte pellets were washed three times with ice-cold 1X phosphate-buffered saline (PBS) pH 7.4, by centrifugation at 2,500g for 10 min at 4 °C. Subsequently, the pellets were resuspended in an equal volume of optimized lysis buffer comprising 1X PBS, 5% SDS (Merck Millipore, Germany), and 1% Triton X-100 (Puregene, USA), supplemented with a protease inhibitor cocktail (cOmplete™, Roche, USA). Following three freeze–thaw cycles, the lysates were clarified by centrifugation at 15,000g for 30 min at 4 °C. The resulting supernatants were collected for subsequent ELISA and Western blot analyses.

4.4 Detection of native PfEXP1 in in vitro-cultured *P. falciparum* lysates

Native PfEXP1 (nPfEXP1) was detected in in vitro-cultured *P. falciparum* lysates using dot blot and Western blot assays with pAb-PfEXP1, as detailed in supplementary methods section **1.4**. For dot blot analysis, lysates corresponding to 4×10^5, 2×10^5, 1×10^5, and 1×10^4 parasites were spotted onto 0·45 µm nitrocellulose membranes using a Bio-Dot SF apparatus (Bio-Rad, USA). For Western blotting, lysates corresponding to 2×10^7, 2×10^6, 4×10^5, 1×10^5, and 1×10^4 parasites were resolved by 12% SDS-PAGE and transferred onto nitrocellulose membranes. Membranes were blocked with 5% skimmed milk in PBS for 2 h at room temperature, followed by incubation with pAb-PfEXP1 (1:2,500) for 2 h. After washing with PBS containing 0·05% Tween-20 (PBST), membranes were incubated with HRP-conjugated goat anti-rabbit IgG (1:10,000; Invitrogen, USA) for 1 h. Immunoreactive signals were developed using Clarity™ Western ECL substrate (Bio-Rad, USA) and visualized using a Western blot imaging system (Azure Biosystems, USA). Recombinant PfEXP1 (100 ng) was included as a positive control. The abundance of nPfEXP1 in parasite lysates was estimated separately by indirect ELISA using an rPfEXP1-derived standard curve. These values were expressed as semiquantitative rPfEXP1-equivalent amounts and were not interpreted as absolute nPfEXP1 concentrations or Western blot-derived limits of detection.

4.5 Index and comparator assays

PfHRP2 is an established diagnostic biomarker for *P. falciparum* malaria, widely employed in lateral-flow RDTs owing to its generally high diagnostic sensitivity and specificity. To facilitate a methodologically consistent comparison between the index (nPfEXP1) and comparator (nPfHRP2) assays, both antigens were evaluated using the same indirect ELISA platform, employing polyclonal anti-PfEXP1 (pAb-PfEXP1) and monoclonal anti-PfHRP2 (mAb-PfHRP2) antibodies, respectively. Although the present evaluation employed a polyclonal antibody-based assay, development of a monoclonal antibody pair for sandwich immunoassay detection of PfEXP1 is underway and will be assessed in subsequent studies. Detailed experimental procedures for both assays are described in the following sections.

4.6 Detection of native PfEXP1 and PfHRP2 in clinical blood samples by indirect ELISA

Native PfEXP1 (nPfEXP1) and PfHRP2 (nPfHRP2) were detected in processed clinical blood samples using indirect ELISA. Briefly, 96-well microtiter plates were coated with 100 µl of each sample per well, in duplicate, and incubated overnight at 4 °C. Plates were blocked with 5% (w/v) bovine serum albumin (BSA) in PBS for 2 h at room temperature. For nPfEXP1

detection, wells were incubated with rabbit polyclonal anti-PfEXP1 antibodies (pAb-PfEXP1; 1:2,500), whereas nPfHRP2 was detected using an in-house-generated mouse monoclonal anti-PfHRP2 antibody (mAb-PfHRP2; clone 3G10F6; SPAN Bioproducts Pvt. Ltd., India; 1:8,000). Primary antibody incubations were performed for 2 h at room temperature, followed by three washes with PBS containing 0·05% Tween-20 (PBST). Subsequently, HRP-conjugated goat anti-rabbit IgG (1:10,000; Invitrogen, USA) or goat anti-mouse IgG (1:10,000; Invitrogen, USA) was added to the respective wells and incubated for 1 h at room temperature. Following three washes with PBST, 50 µl of 3,3′,5,5′-tetramethylbenzidine (TMB; Thermo Scientific, USA) substrate was added, and plates were incubated in the dark for 15 min at room temperature. The reaction was terminated with 50 µl of 0·2 N H_2SO_4, and absorbance was measured at 450 nm. Recombinant PfEXP1 (rPfEXP1; 100 ng) served as a positive control for the PfEXP1 assay, whereas uninfected erythrocyte lysates were included as negative controls.

4.7 Estimation of nPfEXP1 from in vitro cultured *P. falciparum* lysate using mAb-PfEXP1

The generation of mAb-PfEXP1 has been described in detail in supplementary methods section **1.5**. To assess the lowest detectable amount of nPfEXP1 using mAb-PfEXP1, lysates from varying parasite numbers (4×10^6, 2×10^6, 1×10^6, 5×10^5, 2×10^5, 1×10^5, 5×10^4, 2×10^4 and 1×10^4) were loaded onto 12% SDS-PAGE and transferred onto NC membrane. The NC membrane was blocked in PBS containing 5% skimmed milk for 2 hrs. at room temperature (RT) and incubated with mAb-PfEXP1 (3B3B2) (1:10,000) for 2 hrs. After washing with PBS containing 0.05% Tween-20 (PBST), the NC membrane was incubated with HRP-conjugated goat anti-mouse IgG (1:10000) (Dako, Glostrup, Denmark) for 1 hr. After three washes with PBST, the NC membrane was incubated in 1X 10 ml of enhanced in house HRP substrate. For detection of nPfEXP1 in cultured parasites harbouring Pf*hrp2/3* gene deletions (Δ*hrp2* and Δ*hrp2/3*) is described in supplementary methods section **1.6**.

4.8 Statistical analyses

4.8.1 Statistical comparison of *P. falciparum*-positive and control groups

As described in methods section **2.1**, *P. falciparum*-positive samples were categorized into three study-defined parasitaemia groups: low (<5,000 parasites/µl), moderate (5,000–100,000 parasites/µl), and high (>100,000 parasites/µl). The total infected group comprised all *P. falciparum*-positive samples irrespective of parasite density. The control group included malaria-negative individuals from the endemic study site and healthy individuals from non-endemic areas. ELISA absorbance values (OD_{450}) for each infected group were compared

independently with those of the control group using an unpaired, two-tailed Student's t test with Welch's correction for unequal variances. Statistical analyses were performed separately for the PfEXP1 index assay and PfHRP2 comparator assay using GraphPad Prism version 5 (GraphPad Software, USA). A two-sided p value <0·05 was considered statistically significant.

4.8.2 Receiver operating characteristic (ROC) curve and area under the curve (AUC) analysis

Receiver operating characteristic (ROC) curve analysis was performed to evaluate the ability of the PfEXP1 index assay and PfHRP2 comparator assay to discriminate between malaria-negative controls and *P. falciparum*-infected samples. Separate ROC curves were generated for the total infected group and each parasitaemia subgroup (low, moderate, and high) against the control group. The area under the ROC curve (AUC) was calculated to assess the overall discriminatory performance of each assay across the range of possible optical density (OD_{450}) thresholds. All ROC analyses were performed using GraphPad Prism version 5 (GraphPad Software, USA).

4.8.3 Diagnostic performance evaluation of index and comparator tests

To evaluate diagnostic performance, samples were randomly divided into training (70%) and validation (30%) subsets[38]. Optimal assay-specific OD_{450} cutoffs were determined exclusively from the training subset by maximizing Youden's index (J) [$\text{sensitivity} + \text{specificity} - 1$]. The resulting cutoffs were applied without modification to the validation subset to independently assess the diagnostic performance of the PfEXP1 index and PfHRP2 comparator assays. 2 × 2 contingency table matrices were constructed to determine true positives (TP), true negatives (TN), false positives (FP), and false negatives (FN), from which sensitivity, specificity, and balanced accuracy were calculated. Data preprocessing and manipulation were performed in R using the readr, dplyr and pROC packages. The diagnostic performance estimates are presented in **Table 2**.

4.9 Global genetic diversity and haplotype analysis of Pf*exp1*

To compute the genetic variations within the Pf*exp1* (PF3D7_1121600) gene, we utilized the MalariaGEN Pf8 dataset[30], which comprises 33,325 *P. falciparum* field samples collected across 34 malaria-endemic countries, including India. We restricted our downstream analyses to 24,409 quality control (QC)-passed samples, for which annotated VCF files were retrieved from the MalariaGEN Pf8 repository (https://pf8-release.cog.sanger.ac.uk/vcf/index.html) and indexed using bcftools[39]. Variants linked to Pf*exp1* were subsequently extracted based on their genomic coordinates on chromosomes 11 (v3:814,343..818,094(-)), 8 (v3:1373212-1376988(-

)), and 13 (v3:1373212-1376988(-)), respectively. Biallelic variants were filtered and classified into single-nucleotide variants (SNVs) and insertions-deletions (indels) based on the lengths of the reference (REF) and alternate (ALT) alleles. Next, the number of biallelic SNVs within exons, 5′ untranslated (UTR)/upstream regions, 3′ UTR/downstream regions, and introns, was counted. Furthermore, exonic SNVs were functionally categorised as synonymous, missesense/non-synonymous, stop-gained, start-lost, and stop-retained, based on their impact on the protein coding sequence. Distribution summaries were visualized as pie charts and bar graphs using a custom Python script.

Haplotype data for the PfEXP1 gene across the QC-passed samples were obtained from the Pf-HaploAtlas web server (https://pf-haploatlas.streamlit.app/?gene_id=PF3D7_1121600)[32]. Following the retrieval of the population-level summary for 18,970 samples from Pf-HaploAtlas comprising 209, 5851, 886, 162, 3129, 123, 1072, 1724, 5496, and 318 isolates from South America (SA), West Africa (AF-W), Central Africa (AF-C), North-East Africa (AF-NE), East Africa (AF-E), Eastern South Asia (AS-S-E; includes India), Far-Eastern South Asia (AS-S-FE), Western South-East Asia (AS-SE-W), Eastern South-East Asia (AS-SE-E), and Oceania (OC-NG), respectively, the dataset was filtered to retain haplotypes present in a minimum of 10 samples. Custom Python scripts were then used to regenerate the UpSet plots. Global distribution and relative within-population abundance of the PfEXP1 haplotypes, pie chart overlays onto a world map were generated using ggplot2 in R[40]. Separately, PfEXP1 protein haplotypes were estimated using biallelic exonic SNPs for 50 ICMER-MESA (International Centres of Excellence for Malaria Research- Malaria Evolution in South Asia) *P. falciparum* samples collected from four tertiary health care centres spread across the Indian sub-continent (Bavikatte AN et al.- under review)[33,34]. Amino acid substitutions were mapped onto the 162-amino-acid domain structure of the PfEXP1 protein using Python. Four functional regions of PfEXP1 were defined as follows: N-terminal signal peptide (residues ~1–24), the soluble N-terminal lumenal region (residues ~25–80), the single hydrophobic transmembrane domain (residues ~81–102), and the C-terminal cytoplasmic tail (residues ~103–162).

Author contributions

KCP, KV conceptualized the study.

KCP received the funding.

KCP, KV, BD performed project administration.

HLS, BD, VK, PN, NT, SSV, ANB, SC performed the investigation.

KV, KCP, SSV, RS, PKT, SC performed data analysis.

HLS, KV, ANB, SSV wrote the manuscript.

KCP, KV, SSV, SS, PKT, SC, BKN, RD reviewed the manuscript.

KCP and KV has full access to the data and independently verified the underlying data.

Competing interests

The authors declare no conflicts of interest.

Declaration

The Research Integrity Committee (RIC) approved previous versions of this manuscript with RIC no. approval number is RIC-12/2026. The current version has been submitted for RIC approval. This work has been submitted for Indian patent consideration at ICMR Patent Mitra vide application no. 202511056948.

Funding

The study was funded as an intramural research project granted to Dr. Kailash C Pandey by Indian Council of Medical Research, Government of India (VBD/NIMR/Intra/005-ECD-II). All the sample collection and experimental work presented in the study was performed with funds available in the project and no other funding was used.

Data availability

All the data related to experiments have been presented in the manuscript main text and supplementary data. Participants related data can be made available on appropriate request for research.

Acknowledgements

The authors acknowledge health authorities of Jharkhand and Chaibasa including SPO, Stage VBD Consultant, DMO, DVBC, MTS and other staff of NVBDCP, for their help in field studies. The infrastructure support from DHR-MRHRU, Angara, Ranchi is also acknowledged. The authors acknowledge the supportive assistance of Dr. Jatin Kumar, Dr. Bharti Goyal and Shruti Bhatt for her help in the CD spectroscopy experiment.

Declaration of generative AI and AI-assisted technologies in the manuscript preparation process

During the preparation of this work, the author(s) used **Gemini** and **ChatGPT** for language enhancements. The author(s) reviewed and edited the output as needed and take full responsibility for the content of the published article.

5. References

1 WHO. *World Malaria Report 2025*. (World Health Organization, 2025).

2 WHO. Malaria rapid diagnostic test performance: results of WHO product testing of malaria RDTs: round 8 (2016–2018). 17 (WHO, 2018).

3 Ojeniyi, F. D. *et al.* Performance and challenges of malaria rapid diagnostic tests in endemic regions of Africa. *Sci Rep* **15**, 43663, doi:10.1038/s41598-025-97259-x (2025).

4 Li, B. *et al.* Performance of pfHRP2 versus pLDH antigen rapid diagnostic tests for the detection of Plasmodium falciparum: a systematic review and meta-analysis. *Arch Med Sci* **13**, 541-549, doi:10.5114/aoms.2017.67279 (2017).

5 Lynch, E. *et al.* Evaluation of HRP2 and pLDH-based rapid diagnostic tests for malaria and prevalence of pfhrp2/3 deletions in Aweil, South Sudan. *Malar J* **21**, 261, doi:10.1186/s12936-022-04280-w (2022).

6 Alareqi, L. M. Q. *et al.* Field evaluation of a PfHRP-2/pLDH rapid diagnostic test and light microscopy for diagnosis and screening of falciparum malaria during the peak seasonal transmission in an endemic area in Yemen. *Malar J* **15**, 49, doi:10.1186/s12936-016-1103-2 (2016).

7 WHO. *Malaria threats map, WHO*, < https://apps.who.int/malaria/maps/threats/> (2026).

8 Berhane, A. *et al.* Major Threat to Malaria Control Programs by Plasmodium falciparum Lacking Histidine-Rich Protein 2, Eritrea. *Emerg. Infect. Dis.* **24**, 462-470, doi:10.3201/eid2403.171723 (2018).

9 Berhane A, A. K., Mihreteab S, Gresty K, Rogier E, Mohamed S, et al. Major Threat to Malaria Control Programs by Plasmodium falciparum Lacking Histidine-Rich Protein 2, Eritrea. *Emerg Infect Dis.* **24(3)**, 462-470, doi:https://doi.org/10.3201/eid2403.171723 (2018).

10 Agaba, B. B. *et al.* Molecular surveillance reveals the presence of pfhrp2 and pfhrp3 gene deletions in Plasmodium falciparum parasite populations in Uganda, 2017–2019. *Malar J* **19**, 300, doi:10.1186/s12936-020-03362-x (2020).

11 Bredu, D. G. *et al.* Prevalence of Plasmodium falciparum parasites with pfhrp2 exon 2 gene deletion in symptomatic malaria patients across Ghana in 2021. *Malar J* **24**, 170, doi:10.1186/s12936-025-05419-1 (2025).

12 Kojom, L. P. & Singh, V. Prevalence of Plasmodium falciparum field isolates with deletions in histidine-rich protein 2 and 3 genes in context with sub-Saharan Africa and India: a systematic review and meta-analysis. *Malar J* **19**, 46, doi:10.1186/s12936-019-3090-6 (2020).

13 Rogier, E. *et al.* Plasmodium falciparum pfhrp2 and pfhrp3 Gene Deletions and Relatedness to Other Global Isolates, Djibouti, 2019–2020. *Emerg. Infect. Dis.* **28**, 2043-2050, doi:10.3201/eid2810.220695 (2022).
14 Bharti, P. K. *et al.* Prevalence of pfhrp2 and/or pfhrp3 Gene Deletion in Plasmodium falciparum Population in Eight Highly Endemic States in India. *PLoS ONE* **11**, e0157949, doi:10.1371/journal.pone.0157949 (2016).
15 Pati, P., Dhangadamajhi, G., Bal, M. & Ranjit, M. High proportions of pfhrp2 gene deletion and performance of HRP2-based rapid diagnostic test in Plasmodium falciparum field isolates of Odisha. *Malar J* **17(1):394** (2018).
16 Helb, D. A.-O. *et al.* Novel serologic biomarkers provide accurate estimates of recent Plasmodium falciparum exposure for individuals and communities. *Proc. Natl. Acad. Sci. U.S.A.* **112(32):E4438-47** (2015).
17 Kori, L. D., Valecha, N. & Anvikar, A. R. Glutamate dehydrogenase: a novel candidate to diagnose Plasmodium falciparum through rapid diagnostic test in blood specimen from fever patients. *Sci Rep* **10**, 6307, doi:10.1038/s41598-020-62850-x (2020).
18 Rajendra Prasad, M., Anil Kumar, D., Dodwani, E., Singh, S. & Trivedi, V. Antigenic determinant analysis of FIKK Kinase family to identify novel candidates for diagnosis of Plasmodium falciparum. *Microbial Pathogenesis* **209**, 108070, doi:https://doi.org/10.1016/j.micpath.2025.108070 (2025).
19 Dodoo, D. *et al.* Cohort study of the association of antibody levels to AMA1, MSP119, MSP3 and GLURP with protection from clinical malaria in Ghanaian children. *Malar J* **7**, 142, doi:10.1186/1475-2875-7-142 (2008).
20 Mwesigwa, A. *et al.* Plasmodium falciparum genetic diversity and multiplicity of infection based on msp-1, msp-2, glurp and microsatellite genetic markers in sub-Saharan Africa: a systematic review and meta-analysis. *Malar J* **23**, 97, doi:10.1186/s12936-024-04925-y (2024).
21 Vashisht, K. *et al.* Cyclic constrained immunoreactive peptides from crucial P. falciparum proteins: potential implications in malaria diagnostics. *Transl Res* **249**, 28-36, doi:10.1016/j.trsl.2022.06.008 (2022).
22 Iriko, H. *et al.* Plasmodium falciparum Exported Protein 1 is localized to dense granules in merozoites. *Parasitology International* **67**, 637-639, doi:10.1016/j.parint.2018.06.001 (2018).
23 Mesén-Ramírez, P. *et al.* EXP1 is critical for nutrient uptake across the parasitophorous vacuole membrane of malaria parasites. *PLoS Biol* **17**, e3000473, doi:10.1371/journal.pbio.3000473 (2019).
24 Simmons, D., Woollett, G., Bergin-Cartwright, M., Kay, D. & Scaife, J. A malaria protein exported into a new compartment within the host erythrocyte. *EMBO J* **6**, 485-491, doi:10.1002/j.1460-2075.1987.tb04779.x (1987).
25 Heide, J. *et al.* Detection of EXP1-Specific CD4+ T Cell Responses Directed Against a Broad Range of Epitopes Including Two Promiscuous MHC Class II Binders During Acute Plasmodium falciparum Malaria. *Front. Immunol.* **10**, 3037, doi:10.3389/fimmu.2019.03037 (2020).
26 Nessel, T. *et al.* EXP1 is required for organisation of EXP2 in the intraerythrocytic malaria parasite vacuole. *Cellular Microbiology* **22**, doi:10.1111/cmi.13168 (2020).
27 Schulte, S. *et al.* Deciphering the Plasmodium falciparum malaria-specific CD4+ T-cell response: ex vivo detection of high frequencies of PD-1+TIGIT+ EXP1-specific CD4+ T

cells using a novel HLA-DR11-restricted MHC class II tetramer. *Clinical and Experimental Immunology* **207**, 227-236, doi:10.1093/cei/uxab027 (2022).

28 Porter, K. R. *et al.* Immune Response against the Exp-1 Protein of Plasmodium falciparum Results in Antibodies That Cross-React with Human T-Cell Lymphotropic Virus Type 1 Proteins. *Clin Diagn Lab Immunol* **5**, 721-724, doi:10.1128/CDLI.5.5.721-724.1998 (1998).

29 Lisewski, Andreas M. *et al.* Supergenomic Network Compression and the Discovery of EXP1 as a Glutathione Transferase Inhibited by Artesunate. *Cell* **158**, 916-928, doi:10.1016/j.cell.2014.07.011 (2014).

30 Abdel Hamid, M. M. *et al.* Pf8: an open dataset of Plasmodium falciparum genome variation in 33,325 worldwide samples.

31 Zhang, M. A.-O. *et al.* Uncovering the essential genes of the human malaria parasite Plasmodium falciparum by saturation mutagenesis. *Science* **360(6388):eaap7847** (2018).

32 Lee, C. *et al.* Pf-HaploAtlas: an interactive web app for spatiotemporal analysis of Plasmodium falciparum genes. *Bioinformatics* **40**, doi:10.1093/bioinformatics/btae673 (2024).

33 AN, B. *et al. Population genomic structure of Plasmodium falciparum from the Indian sub-continent.* (Under review).

34 Kumar, S. *et al.* Distinct genomic architecture of Plasmodium falciparum populations from South Asia. *Molecular and Biochemical Parasitology* **210**, 1-4, doi:https://doi.org/10.1016/j.molbiopara.2016.07.005 (2016).

35 Gao, Y., Huang, X., Zhu, Y. & Lv, Z. A brief review of monoclonal antibody technology and its representative applications in immunoassays. *J Immunoassay Immunochem* **39(4):351-364** (2018).

36 Poti, K. E. *et al.* In vivo compartmental kinetics of Plasmodium falciparum histidine-rich protein II in the blood of humans and in BALB/c mice infected with a transgenic Plasmodium berghei parasite expressing histidine-rich protein II. *Malar J* **18(1):78** (2019).

37 Cohen, J. F. *et al.* STARD 2015 guidelines for reporting diagnostic accuracy studies: explanation and elaboration. *BMJ Open* **6**, e012799, doi:10.1136/bmjopen-2016-012799 (2016).

38 Dobbin, K. K. & Simon, R. M. Optimally splitting cases for training and testing high dimensional classifiers. *BMC Med Genomics* **Apr 8;4:31**, doi:doi: 10.1186/1755-8794-4-31 (2011).

39 Danecek, P. *et al.* Twelve years of SAMtools and BCFtools. *GigaScience* **10**, doi:10.1093/gigascience/giab008 (2021).

40 Wickham, H. ggplot2: Elegant Graphics for Data Analysis. *Springer-Verlag New York* (2016).

41 Amoah, L. E. *et al.* Contribution of P. falciparum parasites with Pfhrp 2 gene deletions to false negative PfHRP 2 based malaria RDT results in Ghana: A nationwide study of symptomatic malaria patients. *PLoS ONE* **15**, e0238749, doi:10.1371/journal.pone.0238749 (2020).

42 Molina - de la Fuente, I. *et al.* Deletion patterns, genetic variability and protein structure of pfhrp2 and pfhrp3: implications for malaria rapid diagnostic test in Amhara region, Ethiopia. *Malar J* **21**, 287, doi:10.1186/s12936-022-04306-3 (2022).

43 Fontecha, G. *et al.* Deletions of pfhrp2 and pfhrp3 genes of Plasmodium falciparum from Honduras, Guatemala and Nicaragua. *Malar J* **17**, 320, doi:10.1186/s12936-018-2470-7 (2018).

44 Eyong, E. M. *et al.* Plasmodium falciparum histidine-rich protein 2 and 3 gene deletion in the Mount Cameroon region. *IJID Regions* **3**, 300-307, doi:https://doi.org/10.1016/j.ijregi.2022.05.006 (2022).

Supplementary data

The supplementary data is available as a separate document containing supplementary methods, results, tables and figures.

6. Figure legends

Figure 1. Characterization of PfEXP1 sequence conservation, structural features, and stage-specific expression. (A) Multiple sequence alignment of EXP1 orthologues from *P. falciparum*, *P. vivax*, *P. ovale*, *P. malariae*, and *P. knowlesi*, illustrating conserved domain architecture comprising the signal peptide (SP), random-coil (RC), and α-helical regions. The 25-amino-acid PfEXP1-specific C-terminal region (residues 129–154), corresponding to the selected epitope, is highlighted in red. **(B)** Surface representations of the predicted PfEXP1 and PvEXP1 structures. The PfEXP1-specific epitope (NGEPNAGPQVTAQDVTPEQPQGDDN) is surface-exposed and adopts an extended conformation in the predicted PfEXP1 structure. Structures were predicted using AlphaFold3 and visualized in PyMOL. **(C)** SDS-PAGE analysis (12% gel) of size-exclusion chromatography (SEC)-purified recombinant PfEXP1 (rPfEXP1), showing a predominant band at approximately 23 kDa. **(D)** Thermal denaturation profile of purified rPfEXP1 determined by circular dichroism (CD) spectroscopy, showing changes in ellipticity (mdeg) with increasing temperature. **(E)** Immunoblot detection of rPfEXP1 using rabbit anti-PfEXP1 polyclonal antibodies, showing a specific immunoreactive band at approximately 23 kDa. **(F)** Immunoblot detection of native PfEXP1 in lysates from ring-, trophozoite-, and schizont-stage *P. falciparum*, using rabbit anti-PfEXP1 polyclonal antibodies (3 µg of lysate per lane). **(G)** Preliminary dot-blot analysis of rPfEXP1 to assess its qualitative detection limit using rabbit anti-PfEXP1 polyclonal antibodies.

Figure 2. Comparative Western blot analysis of the detection limits of native PfEXP1 in laboratory and field isolates of *Plasmodium falciparum*. (A) Serially diluted lysates of erythrocytes infected with the laboratory strain *P. falciparum* 3D7 were separated by SDS–PAGE and immunoblotted using a rabbit polyclonal anti-PfEXP1 antibody. **(B)** Serially diluted lysates of erythrocytes infected with the culture adapted field isolate *P. falciparum* JDP8 (PfJDP8) were similarly analysed using the rabbit polyclonal anti-PfEXP1 antibody.

Figure 3. Comparative ELISA-based detection of native PfEXP1 and PfHRP2 in clinical blood samples. Native PfEXP1 **(A)** and PfHRP2 **(B)** were detected by indirect ELISA in blood samples from healthy controls and patients with *P. falciparum* infection, stratified by parasite density into low (<5,000 parasites/µl), moderate (5,000–100,000 parasites/µl), and high (>100,000 parasites/µl) groups. ELISA signals were compared across the groups to assess the detectability of nPfEXP1 relative to PfHRP2 at different levels of parasitaemia.

Figure 4. Receiver operating characteristic (ROC) curve analysis of the PfEXP1 and PfHRP2 assays. ROC curves showing the ability of the PfEXP1 **(A)** and PfHRP2 (B) assays to discriminate between healthy controls and *P. falciparum*-infected patients stratified by parasite density: low (<5,000 parasites/µl), moderate (5,000–100,000 parasites/µl), and high (>100,000 parasites/µl). ROC curves and corresponding area under the curve (AUC) values and performance metrics were generated using GraphPad Prism.

Figure 5. Detection of native PfEXP1 in *Plasmodium falciparum*-infected erythrocyte lysates using monoclonal anti-PfEXP1 antibodies. (A) Western blot analysis showing the detection of native PfEXP1 in lysates prepared from *P. falciparum* 3D7-infected erythrocytes at different parasite densities, using TMB substrate **(Table S4)**. **(B)** Western blot analysis of serially diluted *P. falciparum* 3D7-infected erythrocyte lysates **(Table S5)**, with recombinant PfEXP1 (rPfEXP1) included as a positive control. No cross-reactive signal was detected in the *P. vivax*-infected patient lysate when the blot was developed using an ECL chemiluminescence substrate. In both panels, proteins were separated by SDS-PAGE and probed with the monoclonal anti-PfEXP1 antibody, followed by an HRP-conjugated anti-mouse secondary antibody. Detection was performed using the indicated substrates.

Figure 6. Detection of native PfEXP1 and confirmation of Pf*hrp2* deletion in *Plasmodium falciparum* parasite lines. Western blot analysis using the 3B3B2 anti-PfEXP1 monoclonal antibody demonstrated the presence of native PfEXP1 in Pf3D7, PfJDP8, Δ*hrp2*, and Δ*hrp2/3* parasite lines (10 µg of parasite lysate per lane), whereas no detectable signal was observed in uninfected red blood cell (uRBC) lysate. Inset: PCR amplification using Pf*hrp2*-specific One-step primers confirmed the presence of Pf*hrp2* in Pf3D7 and PfJDP8, while no amplification was detected in the Δ*hrp2* and Δ*hrp2/3* lines, confirming the absence of the Pf*hrp2* target sequence in these mutants.

Figure 7: Global population genetic diversity and protein polymorphisms of PfEXP1. (A) Genomic distribution of biallelic SNVs identified in the PfEXP1 genomic locus by MalariaGEN Pf8. Variants were classified according to their genomic location, including exonic, 3′ UTR/downstream, 5′ UTR/upstream, and intronic regions. The number of variants and their corresponding percentages are indicated above each bar. UTR = Untranslated region. **(B)** Functional annotation of biallelic, exonic SNVs within PfEXP1. Variants were categorized based on their predicted effects on protein coding sequence, including missense, synonymous, stop-gained, start-lost, and stop-retained mutations. The number of variants and their corresponding percentages are indicated above each bar. Non-syn = Non-synonymous. **(C)** Schematic representation of the PfEXP1 protein showing the positions of naturally occurring amino acid substitutions identified in the MalariGEN Pf8 dataset. Conserved domains, including the predicted transmembrane region, are indicated along the protein sequence. **(D)** Frequency distribution of PfEXP1 protein haplotypes identified across the MalariaGEN Pf8 dataset by Pf-HaploAtlas. The lower panel of the UpSet plot indicates the amino acid composition of PfEXP1 protein haplotypes that were found in at least 10 QC-passed Pf8 samples. Each vertical column represents a unique haplotype, with dots indicating amino acid substitutions relative to the reference *P. falciparum* 3D7 sequence. The y-axis lists polymorphic amino acid positions, and connected substitutions define the mutational profile of each haplotype. The upper panel shows the number of isolates belonging to each haplotype, while the stacked bar plot in the middle panel illustrates the geographic distribution of each haplotype across malaria-endemic regions, including South America (SA), West Africa (AF-W), Central Africa (AF-C), North-East Africa (AF-NE), East Africa (AF-E), Eastern South Asia (AS-S-E; includes India), Far-Eastern South Asia (AS-S-FE), Western South-East Asia (AS-SE-W), Eastern South-East Asia (AS-SE-E), and Oceania (OC-NG). The reference laboratory strains Dd2, IT, HB3, 7G8, GB4, and 3D7 are included for comparison. **(E)** Global geographic distribution of PfEXP1 protein haplotypes. Pie charts indicate the relative frequency of individual PfEXP1 haplotypes within parasite populations from different malaria-endemic regions as defined in part D; refer to the inset for haplotype colour labels. Note that pie size is not proportional to the number of isolates analyzed from each geographic location.

Tables and Figures

Table 1: Global distribution of reported Pf*hrp2* and Pf*hrp3* gene deletions

	Types of deletions			
Country	**Pf*hrp2***	**Pf*hrp3***	**Pf*hrp2/3***	**References**
Ghana	Exon2> Exon1-2	Exon2> Exon1-2	---	[41]
Ghana	Exon 2	---	---	[11]
Ethiopia	Exon1-2>Exon 1	Exon 2> Exon 1-2	---	[42]
Equatorial Guinea	Exon 2	---	---	[42]
Honduras	Exon 1-2	---	---	[42]
India	Exon1-2 and Exon 2	Exon1-2 and Exon 2	---	[14,15]
Guatemala	Exon 1-2	Exon 1-2	---	[43]
Nicaragua	Exon 1-2 whole gene deletion	Exon 1-2 deletion high	---	[43]
Cameroon	Exon 2 deletions	---	---	[44]

Table 2: Parasite density-stratified 2×2 contingency tables for the PfEXP1 index and PfHRP2 comparator assays

	Groups	N	Malaria positive	Malaria negative	True positive (TP)	False negative (FN)	True negative (TN)	False positive (FP)
PfEXP1 [Index test]	**Training subset [70%]**	140	84	56	76	8	43	13
	Validation subset [30%]	***61***	***37***	***24***	***32***	***5***	***14***	***10***
PfHRP2 [Comparator test]	**Training subset [70%]**	140	84	56	84	0	51	5
	Validation subset [30%]	***61***	***37***	***24***	***35***	***2***	***21***	***3***

Table 3: Diagnostic performance of PfEXP1 and PfHRP2 indirect ELISA assays in clinical samples using (70:30) training–validation subsets

	PfEXP1 [Index]		**PfHRP2 [Comparator]**	
Parameters	**Training subset [CI]**	***Validation subset [CI]***	**Training subset [CI]**	***Validation subset [CI]***
Sensitivity	**90% [82-96]**	***86% [71-95]***	**100% [96-100]**	***95% [82-99]***
Specificity	**77% [64-87]**	***58% [37-78]***	**91% [81-96]**	***88% [69-96]***
Positive Predictive Value	**85% [76-92]**	***76% [61-88]***	**94% [88-98]**	***92% [79-97]***
Negative Predictive Value	**84% [71-93]**	***74% [49-91]***	**100% [93-100]**	***91% [73-98]***
Balanced accuracy	**85%**	***75%***	**95%**	***91%***

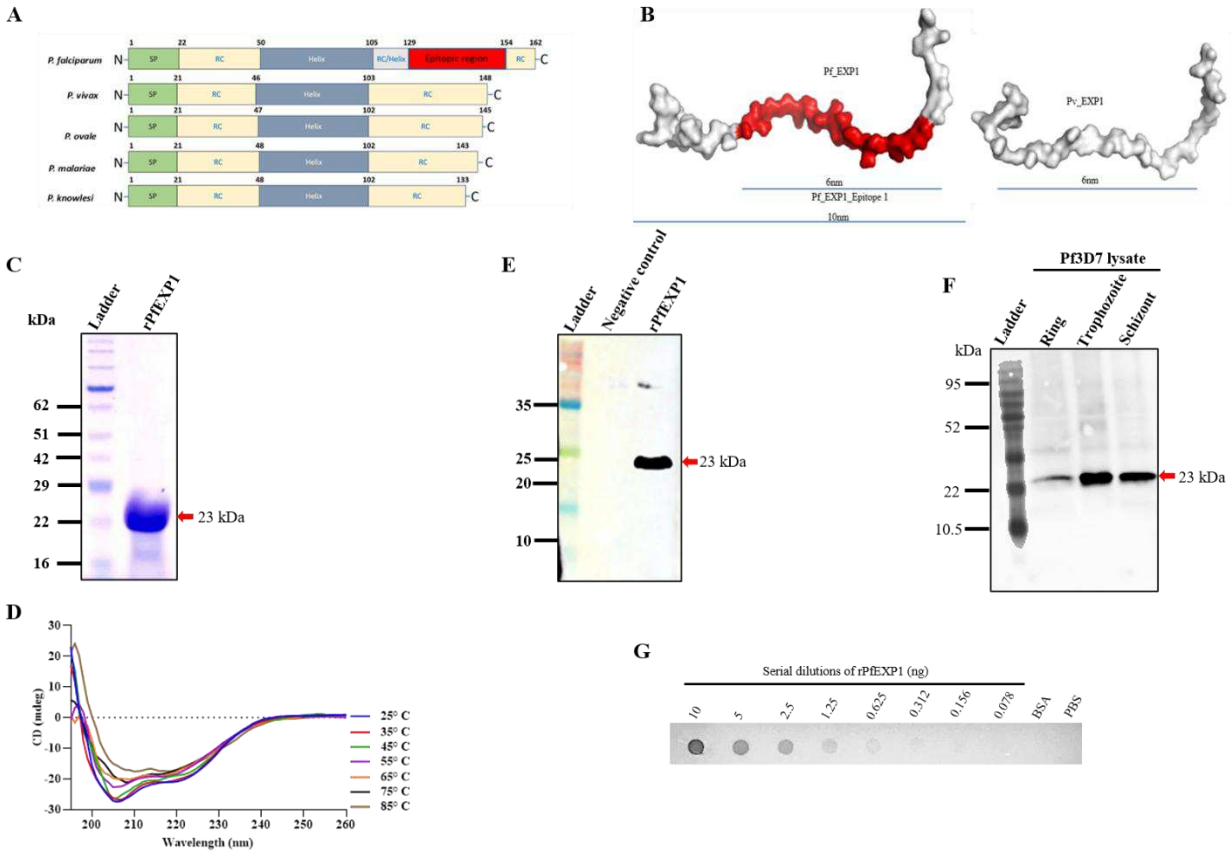


Figure 1. Characterization of PfEXP1 sequence conservation, structural features, and stage-specific expression. (A) Multiple sequence alignment of EXP1 orthologues from *P. falciparum*, *P. vivax*, *P. ovale*, *P. malariae*, and *P. knowlesi*, illustrating conserved domain architecture comprising the signal peptide (SP), random-coil (RC), and α-helical regions. The 25-amino-acid PfEXP1-specific C-terminal region (residues 129–154), corresponding to the selected epitope, is highlighted in red. **(B)** Surface representations of the predicted PfEXP1 and PvEXP1 structures. The PfEXP1-specific epitope (NGEPNAGPQVTAQDVTPEQPQGDDN) is surface-exposed and adopts an extended conformation in the predicted PfEXP1 structure. Structures were predicted using AlphaFold3 and visualized in PyMOL. **(C)** SDS-PAGE analysis (12% gel) of size-exclusion chromatography (SEC)-purified recombinant PfEXP1 (rPfEXP1), showing a predominant band at approximately 23 kDa. **(D)** Thermal denaturation profile of purified rPfEXP1 determined by circular dichroism (CD) spectroscopy, showing changes in ellipticity (mdeg) with increasing temperature. **(E)** Immunoblot detection of rPfEXP1 using rabbit anti-PfEXP1 polyclonal antibodies, showing a specific immunoreactive band at approximately 23 kDa. **(F)** Immunoblot detection of native PfEXP1 in lysates from ring-, trophozoite-, and schizont-stage *P. falciparum*, using rabbit anti-PfEXP1 polyclonal antibodies (3 µg of lysate per lane). **(G)** Preliminary dot-blot analysis of rPfEXP1 to assess its qualitative detection limit using rabbit anti-PfEXP1 polyclonal antibodies.

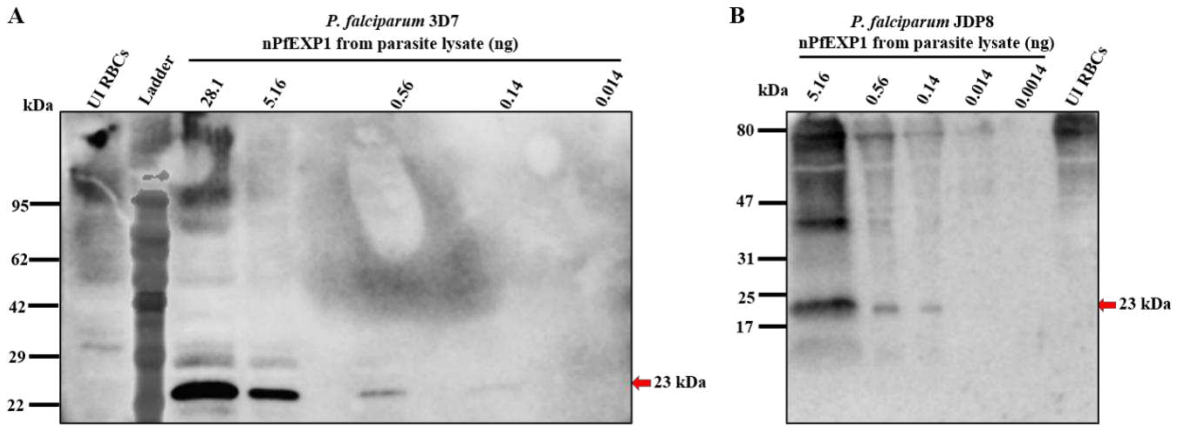


Figure 2. Comparative Western blot analysis of the detection limits of native PfEXP1 in laboratory and field isolates of *Plasmodium falciparum*. (A) Serially diluted lysates of erythrocytes infected with the laboratory strain *P. falciparum* 3D7 were separated by SDS–PAGE and immunoblotted using a rabbit polyclonal anti-PfEXP1 antibody. **(B)** Serially diluted lysates of erythrocytes infected with the culture adapted field isolate *P. falciparum* JDP8 (PfJDP8) were similarly analysed using the rabbit polyclonal anti-PfEXP1 antibody.

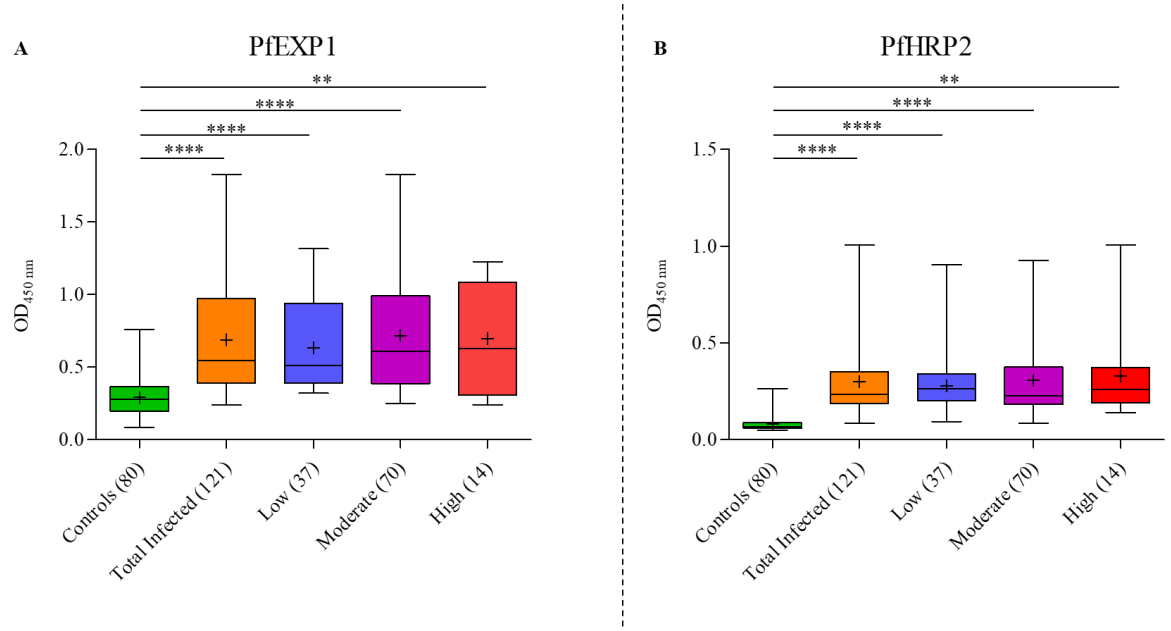


Figure 3. Comparative ELISA-based detection of native PfEXP1 and PfHRP2 in clinical blood samples. Native PfEXP1 **(A)** and PfHRP2 **(B)** were detected by indirect ELISA in blood samples from healthy controls and patients with *P. falciparum* infection, stratified by parasite density into low (<5,000 parasites/µl), moderate (5,000–100,000 parasites/µl), and high (>100,000 parasites/µl) groups. ELISA signals were compared across the groups to assess the detectability of nPfEXP1 relative to PfHRP2 at different levels of parasitaemia.

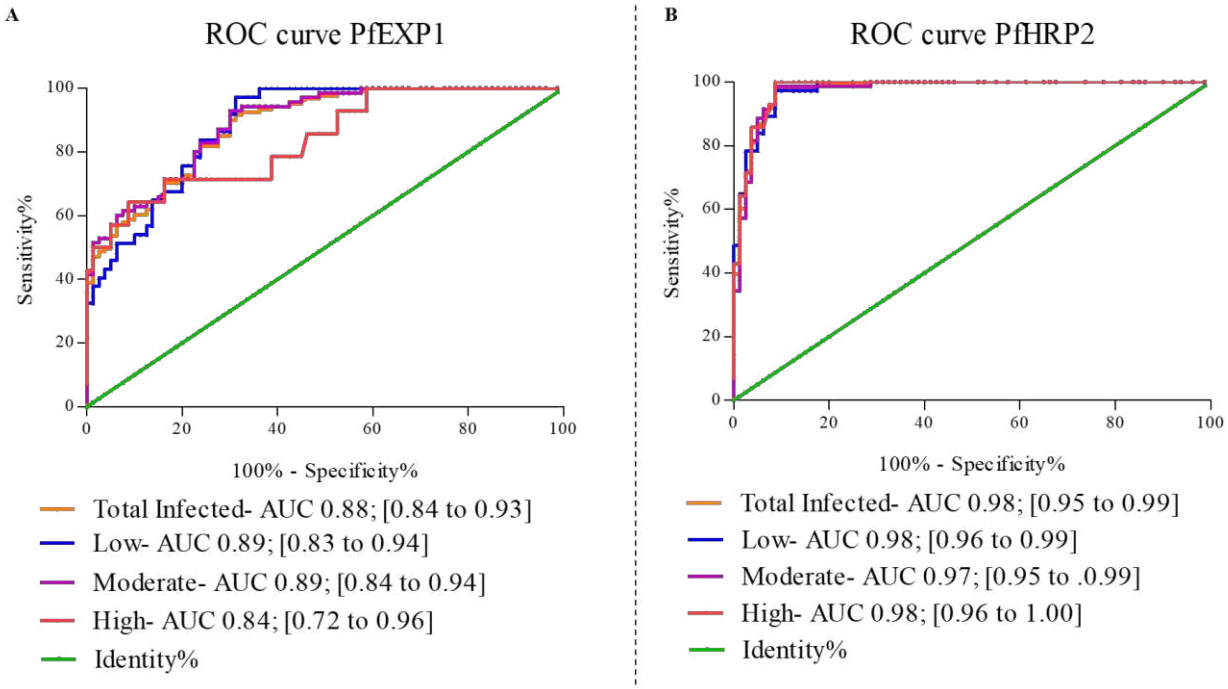


Figure 4. Receiver operating characteristic (ROC) curve analysis of the PfEXP1 and PfHRP2 assays. ROC curves showing the ability of the PfEXP1 **(A)** and PfHRP2 (B) assays to discriminate between healthy controls and *P. falciparum*-infected patients stratified by parasite density: low (<5,000 parasites/µl), moderate (5,000–100,000 parasites/µl), and high (>100,000 parasites/µl). ROC curves and corresponding area under the curve (AUC) values and performance metrics were generated using GraphPad Prism.

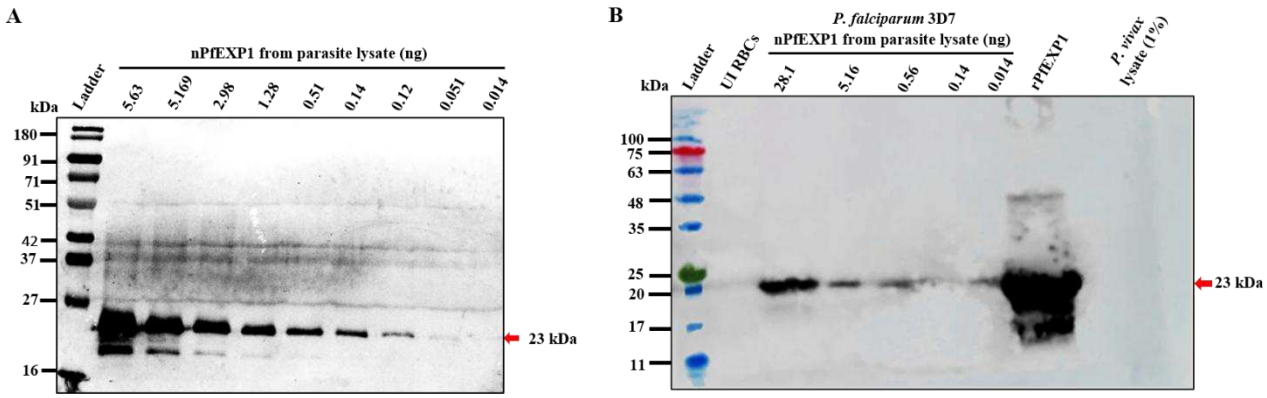


Figure 5. Detection of native PfEXP1 in *Plasmodium falciparum*-infected erythrocyte lysates using monoclonal anti-PfEXP1 antibodies. (A) Western blot analysis showing the detection of native PfEXP1 in lysates prepared from *P. falciparum* 3D7-infected erythrocytes at different parasite densities, using TMB substrate **(Table S4)**. **(B)** Western blot analysis of serially diluted *P. falciparum* 3D7-infected erythrocyte lysates **(Table S5)**, with recombinant PfEXP1 (rPfEXP1) included as a positive control. No cross-reactive signal was detected in the *P. vivax*-infected patient lysate when the blot was developed using an ECL chemiluminescence substrate. In both panels, proteins were separated by SDS-PAGE and probed with the monoclonal anti-PfEXP1 antibody, followed by an HRP-conjugated anti-mouse secondary antibody. Detection was performed using the indicated substrates.

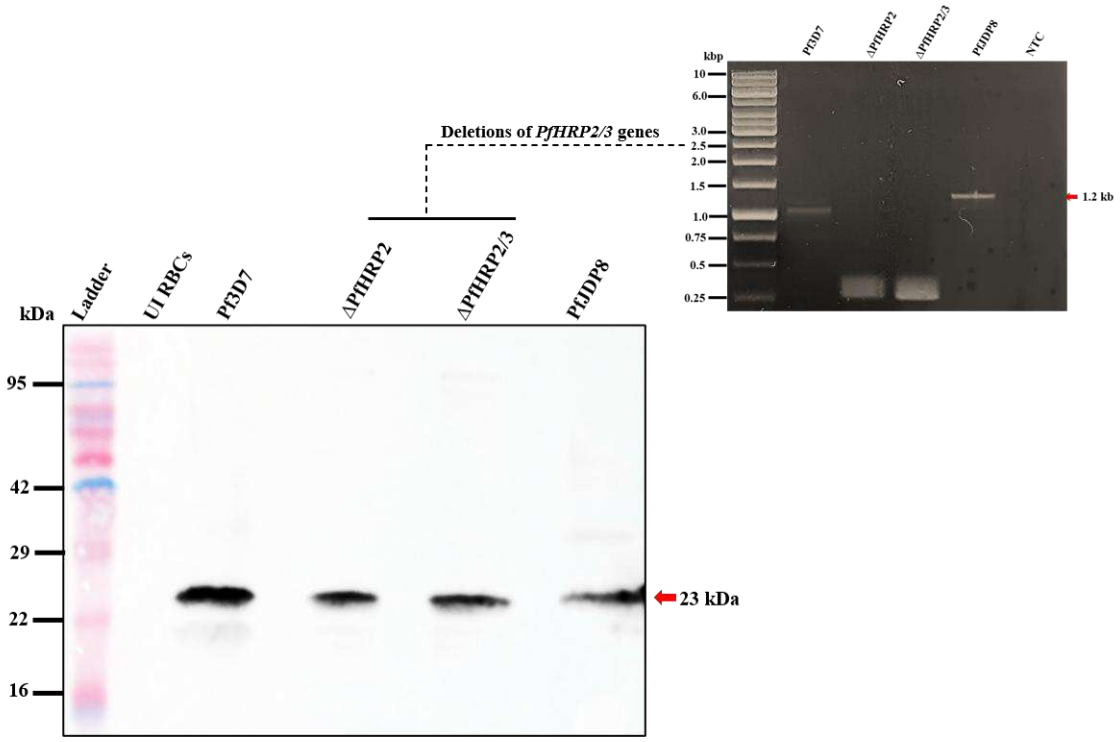
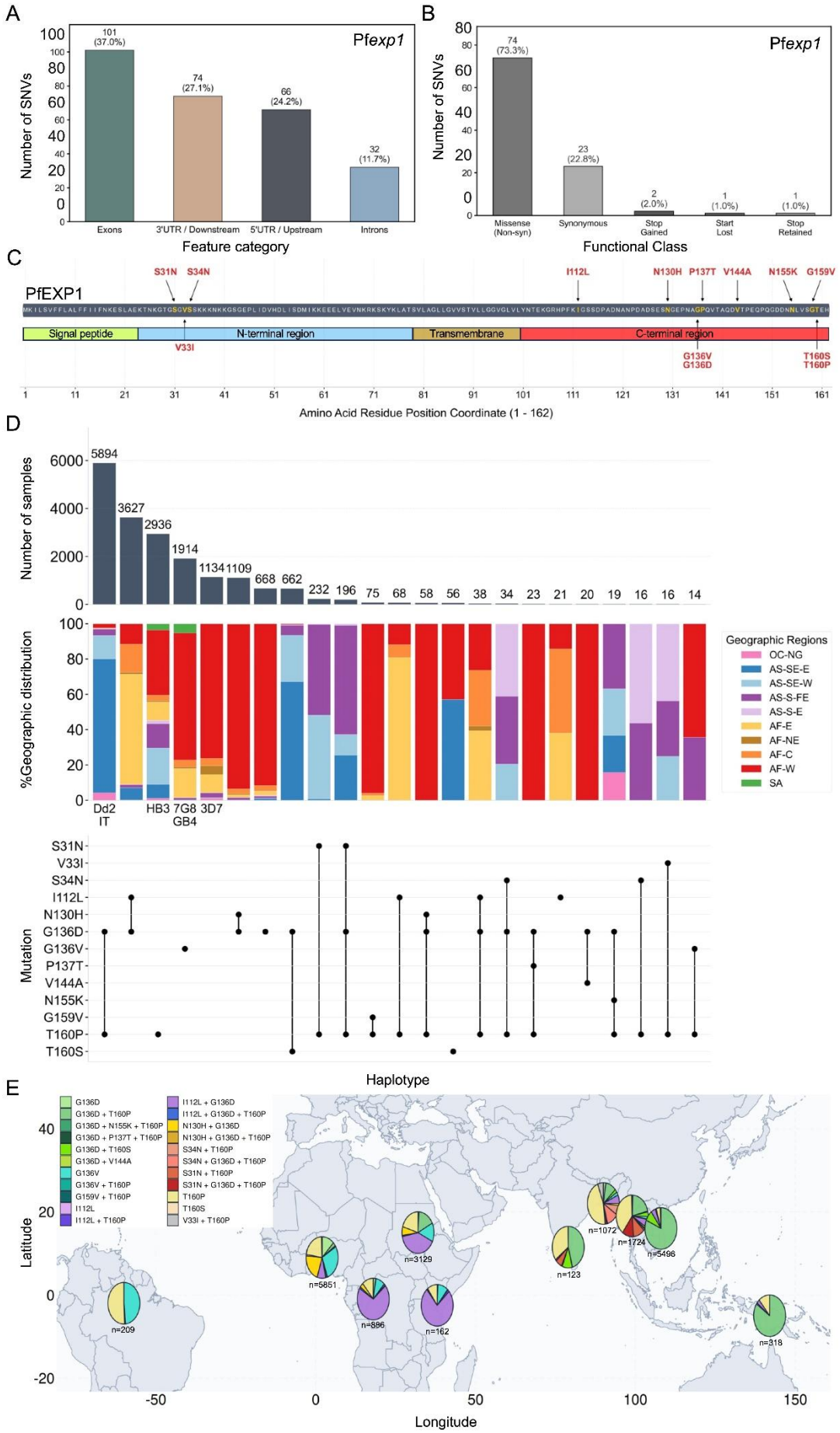


Figure 6. Detection of native PfEXP1 and confirmation of Pf*hrp2* deletion in *Plasmodium falciparum* parasite lines. Western blot analysis using the 3B3B2 anti-PfEXP1 monoclonal antibody demonstrated the presence of native PfEXP1 in Pf3D7, PfJDP8, Δ*hrp2*, and Δ*hrp2/3* parasite lines (10 µg of parasite lysate per lane), whereas no detectable signal was observed in uninfected red blood cell (uRBC) lysate. Inset: PCR amplification using Pf*hrp2*-specific One-step primers confirmed the presence of Pf*hrp2* in Pf3D7 and PfJDP8, while no amplification was detected in the Δ*hrp2* and Δ*hrp2/3* lines, confirming the absence of the Pf*hrp2* target sequence in these mutants.



1 **Figure 7: Global population genetic diversity and protein polymorphisms of PfEXP1. (A)** Genomic

distribution of biallelic SNVs identified in the PfEXP1 genomic locus by MalariaGEN Pf8. Variants were classified according to their genomic location, including exonic, 3′ UTR/downstream, 5′ UTR/upstream, and intronic regions. The number of variants and their corresponding percentages are indicated above each bar. UTR = Untranslated region. **(B)** Functional annotation of biallelic, exonic SNVs within PfEXP1. Variants were categorized based on their predicted effects on protein coding sequence, including missense, synonymous, stop-gained, start-lost, and stop-retained mutations. The number of variants and their corresponding percentages are indicated above each bar. Non-syn = Non-synonymous. **(C)** Schematic representation of the PfEXP1 protein showing the positions of naturally occurring amino acid substitutions identified in the MalariGEN Pf8 dataset. Conserved domains, including the predicted transmembrane region, are indicated along the protein sequence. **(D)** Frequency distribution of PfEXP1 protein haplotypes identified across the MalariaGEN Pf8 dataset by Pf-HaploAtlas. The lower panel of the UpSet plot indicates the amino acid composition of PfEXP1 protein haplotypes that were found in at least 10 QC-passed Pf8 samples. Each vertical column represents a unique haplotype, with dots indicating amino acid substitutions relative to the reference *P. falciparum* 3D7 sequence. The y-axis lists polymorphic amino acid positions, and connected substitutions define the mutational profile of each haplotype. The upper panel shows the number of isolates belonging to each haplotype, while the stacked bar plot in the middle panel illustrates the geographic distribution of each haplotype across malaria-endemic regions, including South America (SA), West Africa (AF-W), Central Africa (AF-C), North-East Africa (AF-NE), East Africa (AF-E), Eastern South Asia (AS-S-E; includes India), Far-Eastern South Asia (AS-S-FE), Western South-East Asia (AS-SE-W), Eastern South-East Asia (AS-SE-E), and Oceania (OC-NG). The reference laboratory strains Dd2, IT, HB3, 7G8, GB4, and 3D7 are included for comparison. **(E)** Global geographic distribution of PfEXP1 protein haplotypes. Pie charts indicate the relative frequency of individual PfEXP1 haplotypes within parasite populations from different malaria-endemic regions as defined in part D; refer to the inset for haplotype colour labels. Note that pie size is not proportional to the number of isolates analyzed from each geographic location.

Supplementary Files

This is a list of supplementary files associated with this preprint. Click to download.

- FinalSuppementarydata02.11.26.docx
- SupplementaryFiguresfullgelblots.pdf